Vienna Congress on Recent Advances in
Earthquake Engineering and Structural Dynamics 2013 (VEESD 2013)
C. Adam, R. Heuer, W. Lenhardt & C. Schranz (eds)
28-30 August 2013, Vienna, Austria
Paper No. 94

Towards a static pushover approximation of peak floor accelerations

L. Moschen[1], D. Vamvatsikos[2], C. Adam[1]

[1] Unit of Applied Mechanics, University of Innsbruck, Innsbruck, Austria
[2] School of Civil Engineering, National Technical University of Athens, Athens, Greece

Abstract. The potential basis of a simplified methodology for estimating the inelastic peak floor acceleration demand (PFA) of multi-story buildings subjected to seismic excitation is explored. Inelastic single-degree-of-freedom (SDOF) oscillators are used to find a relation between the lateral strength and the inelastic acceleration demand. Effects of positive as well as negative post yielding stiffness and different damping types are assessed. Using regression analysis, a simplified approach is proposed to estimate inelastic acceleration demands for use within a probabilistic framework. Based on a fundamental mode approximation an existing approach for predicting elastic PFA demands is extended to inelastic multi-story structures. Pros and cons of this methodology are discussed, and further developments are recommended.

Keywords: Peak floor acceleration; Incremental dynamic analysis; Modal superposition; Regression analysis

1 INTRODUCTION

Several procedures have been developed to estimate the peak floor acceleration (PFA) demand in elastic buildings under earthquake excitation. Employing either an equivalent lateral force procedure (ELFP) or modal response spectrum analysis López-García et al. (2008) suggested a method to estimate modal spectral acceleration demands. Transforming the modal response quantities into the geometric domain using the well-known square-root-of-square-sum (SRSS) method leads to PFA estimates. Taghavi and Miranda (2008) introduced an extended modal combination method, based on a modified complete-quadratic-combination (CQC) rule (Wilson et al. 1981). They quantified the correlation between peak ground acceleration (PGA) and modal floor acceleration, and proposed improved correlation coefficients. In ATC-58-1 (2012) estimation procedures are codified for elastic behaviour of different types of load bearing structures, such as moment resisting as well as braced frames. These procedures even allow the assessment of the central tendency and dispersion of the PFA for probabilistic studies. In a further study, Chaudhuri and Hutchinson (2004) compare actual PFA demands in inelastic buildings with recommendations in actual design standards (FEMA P-750 2009, UBC 1997). They obtained a nonlinear distribution of the PFA over the building height, and based on these outcomes they propose an S-shaped distribution. However, standards propose a linear variation of the PFA, thus, underestimating this response quantity in most of the building stories. Generally, recommendations and codes in the US (FEMA P-750 2009, UBC 1997, IBC 2012) refer to the standard *ASCE/SEI 7-05* (ASCE 2006). The European earthquake design standard (EN 1998-1 2011) does not provide the professional engineer with any information regarding PFA. Recently, within the Global Earthquake Model (GEM) (Porter et al. 2012) an approach was developed for elastic buildings, based on a first mode approximation with explicit consideration of the level of PGA. Results show that the proposed procedure may lead to accurate enough results if the structure is not too tall and behaves elastically.

All the aforementioned methodologies require elastic structural behaviour. The only alternative for use in the inelastic range is the cumbersome application of nonlinear dynamic analysis. The motivation for this paper is to introduce a middle path, resembling the application of nonlinear static procedure by using an analytical relation between the intensity of the record and the inelastic acceleration demand of a single-degree-of-freedom (SDOF) system, which is comparable with the methodology introduced by Ruiz-García and Miranda (2007) for displacement demands. To keep the application as simple as possible the single-mode GEM approach is modified taking into account nonlinear structural behaviour. Relations derived by means of regression analysis on acceleration demands of nonlinear SDOF systems are used to predict PFA demands of inelastic multi-degree-of-freedom (MDOF) buildings. As an example, the extended procedure is applied to a six-story generic frame and subsequently evaluated.

2 SYSTEM RESPONSE STUDY

This section contains several studies of peak acceleration demands of inelastic SDOF systems as well as inelastic MDOF structures seen through incremental dynamic analysis (IDA) (Vamvatsikos and Cornell 2005). All mechanical systems are subjected to the 44 records of the ATC63 far-field record set (FEMA P-695 2009).

2.1 Single-degree-of-freedom system analysis

The motivation for studying an inelastic SDOF system with bilinear hysteretic behaviour is to find a simple analytical relationship between the intensity measure (IM), defined by the elastic spectral acceleration S_{ae} , and the corresponding inelastic peak absolute acceleration demand P_{ai} as a function of the system period T. Elastic characteristic structural parameters are the period T (respectively the circular frequency ω) and the damping ratio ζ. Yield strength F_y and kinematic hardening coefficient α characterize the hysteretic properties. Initially, 5% mass-proportional damping and linear elastic-perfectly plastic behaviour (i.e. $\alpha = 0$) is assumed.

2.1.1 Relation between inelastic peak acceleration demand and elastic spectral acceleration

For a given intensity defined by the elastic spectral acceleration S_{ae} the corresponding peak acceleration of the SDOF system P_{ai} is recorded. To generalize the outcomes, both quantities are normalized by means of the corresponding quantities at onset of yield S_{ay} and P_{ay} ,

$$R_e = \frac{S_{ae}}{S_{ay}}, \quad R_i = \frac{P_{ai}}{P_{ay}} \tag{1}$$

resulting in the lateral strength ratio R_e and the peak acceleration demand ratio R_i , respectively. Note that S_{ay} is related to the yield displacement S_{dy} according to

$$S_{ay} = \omega^2 S_{dy} \tag{2}$$

As an example, in Figure 1 R_e is plotted against R_i for an SDOF system with period $T = 1.00$ s subjected to the 44 records of the ATC63 far-field ground motion set. Gray curves are single record IDA curves, and red lines highlight the corresponding median and 16th and 84th percentiles. For $R_e \leq 1$ respectively $R_i \leq 1$ and the plotted relation is linear with unit slope because the oscillator responds elastically. At an R_e value slightly larger than 1.0 the curves exhibit a more or less pronounced kink, and subsequently the relation between R_e and R_i tends to be almost linear, however with increased slope although the response is now inelastic.

Figure 2 depicts the median R_e - R_i relationship as a function of the oscillator period T in the inelastic response domain (i.e. $R_e \geq 1$, $R_i \geq 1$). The considered period range 0.10 s $\leq T \leq$ 3.00 s covers the most common civil engineering structures. For better understanding the contour plot shows the median inelastic peak acceleration demand R_i for a specific period T and lateral strength ratio R_e. In general, short periods return the highest R_i values. Around $T \approx 0.50$ s R_i is a minimum, for periods $T > 0.50$ s R_i increases for given R_e with respect to T. Note the linear trend along the R_e-axis for any specific period.

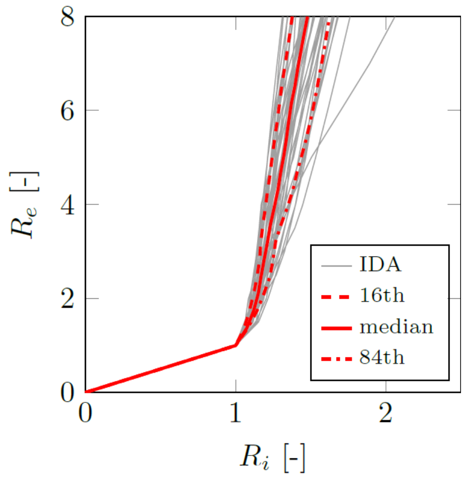

Figure 1. R_e - R_i relation for an SDOF system with period T = 1.00 s.

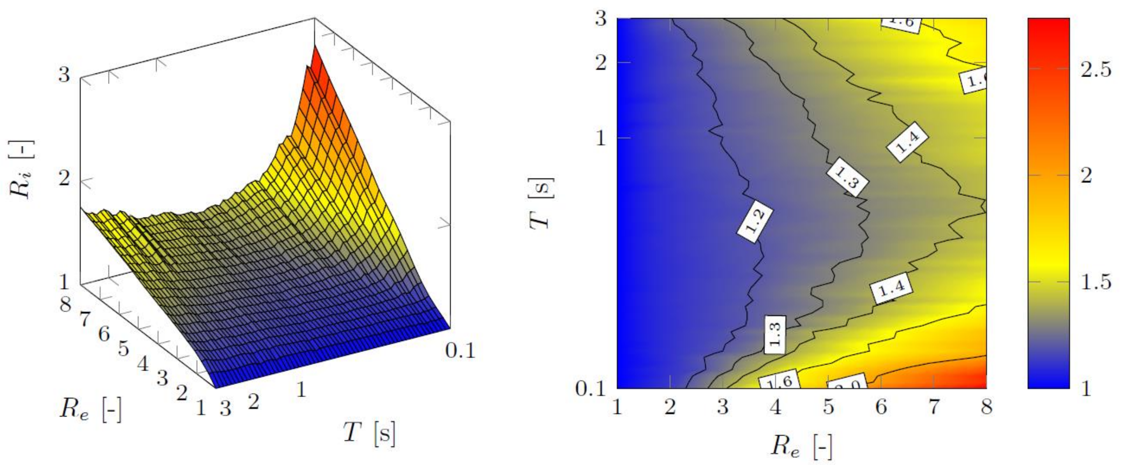

Figure 2. R_e - T - R_i relation (median).

2.1.2 *Central tendency*

Since an almost linear relation between the lateral strength R_e and the inelastic acceleration demand R_i has been revealed, the following analytical equation for the median R_e - T - R_i relation is introduced:

$$\tilde{R}_i(R_e,T) = \begin{cases} R_e & R_e \leq 1 \\ a_1(T)R_e + a_2(T) & R_e > 1 \end{cases} \tag{3}$$

Coefficients a_1 and a_2 define the slope and the intercept along the R_e-axis for given T:

$$a_j(T) = c_{j,1}e^{c_{j,2}\ln(T)} + c_{j,3}e^{c_{j,4}\ln(T)}, \quad j = 1,2 \tag{4}$$

Parameters $c_{j,k}$ are estimated by linear regression analysis and listed in Table 1 for the median.

To quantify the quality of this analytical approximation the relative error with respect to the numerical outcomes, defined as

$$err = \frac{\tilde{R}_i - R_i}{R_i} \tag{5}$$

is evaluated. Figure 3 shows the analytical R_e - T - R_i approximation according to Eq. (3), and the relative error of this approximation. Thereby, a positive error indicates an overestimation of the inelastic acceleration demands. The relative error is largest (i.e. 5%) for R_e close to 1 in the entire period range 0.4 s $\leq T \leq$ 3.0 s in the domain of transition from the linear to the nonlinear regime (see Figure 1). For stiff short period systems errors become also larger along the entire R_e-axis. All other domains exhibit a small error in central tendency.

Table 1. Parameters $c_{j,k}$ to estimate central tendency.

j	$c_{j,1}$	$c_{j,2}$	$c_{j,3}$	$c_{j,4}$
1	0.0031	-1.8756	0.0581	0.4414
2	1.0210	-0.0428	-0.0229	-1.3226

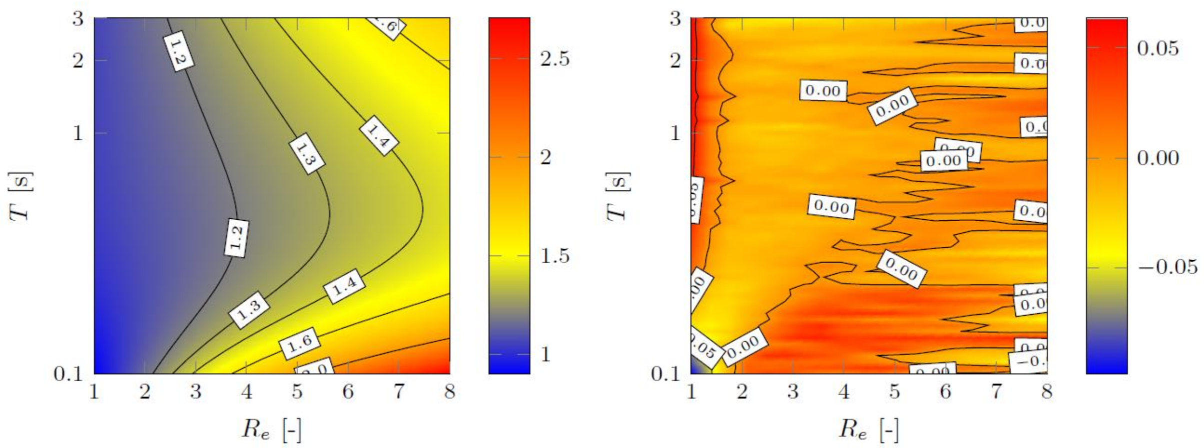

Figure 3. Approximation of median R_e-T-R_i relation (left) and relative error (right).

2.1.3 Dispersion

Due to the record-to-record variability the seismic response is in general lognormally distributed (Chaudhuri and Hutchinson 2004). Therefore, Eqs (3) and (4) approximate also the 16th ($R_{i,16}$) and 84th ($R_{i,84}$) percentiles of the individual inelastic peak acceleration demands R_i, however with different coefficients $a_j(T)$. A linear regression analysis delivers the corresponding parameters $c_{j,k}$ listed in Table 2.

Table 2. Parameters $c_{j,k}$ to estimate dispersion.

	Estimation of 16th percentile values				Estimation of 84th percentile values			
j	$c_{j,1,16}$	$c_{j,2,16}$	$c_{j,3,16}$	$c_{j,4,16}$	$c_{j,1,84}$	$c_{j,2,84}$	$c_{j,3,84}$	$c_{j,4,84}$
1	0.0023	-1.5770	0.0421	0.3585	1.0142	-0.0193	-0.0055	-1.5726
2	0.0186	-1.2873	0.0607	0.8775	1851.6	-0.3286	-1850.6	-0.3288

The measure of dispersion $\tilde{\sigma}$ of a lognormal distributed function is related to the multiplicative standard deviation $\tilde{s}$ according to (Limpert et al. 2001)

$$\tilde{\sigma} = \ln(\tilde{s}) \ , \quad \tilde{s} = \sqrt{\frac{\tilde{R}_{i,84}}{\tilde{R}_{i,16}}} \tag{6}$$

Figure 4 shows both the surface plot and the corresponding contour plot of the dispersion parameter $\tilde{\sigma}$ with respect to R_e and T. For short period systems $T \leq 0.25$ s the dispersion is largest. Systems within the period range $0.25 \text{ s} \leq T \leq 1.50$ s exhibit a very small dispersion.

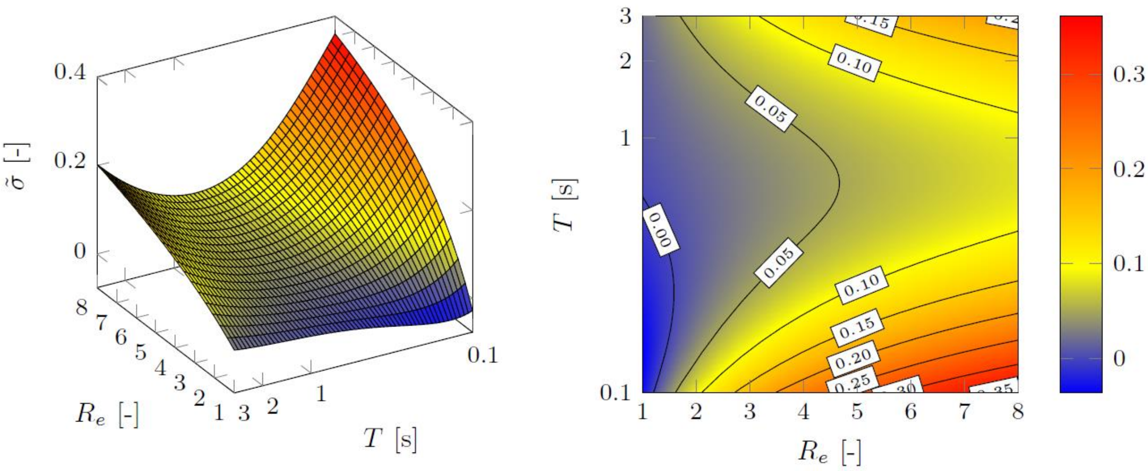

Figure 4. Analytical approximation of the dispersion of the inelastic acceleration demand.

2.1.4 Effect of post-yield hardening and damping

Subsequently, the effect of post-yield hardening on the inelastic acceleration demand of SDOF systems is studied. A 5% damped inelastic SDOF system with period $T = 1.00$ s is subjected to single record IDA. Various hardening coefficients in the range of $\alpha = [0, 0.05, 0.10, 0.20]$ are taken into account. Additionally, for each oscillator both mass- and tangent-stiffness-proportional damping is considered separately to reveal the influence of the underlying viscous damping model on the acceleration response. The blue curve of Figure 5 depicts the acceleration demand for the linear elastic-perfectly plastic oscillator (i.e. $\alpha = 0\%$). It is readily observed that stiffness proportional damping leads in the inelastic response domain to a constant acceleration demand.

This is obvious, because the plastic part of the elastic-plastic stiffness matrix equals the elastic part if the system behaves inelastically. This means that the stiffness equals zero and then, exactly then, damping also equals zero, because damping directly relates to the stiffness. Thus, for inelastic time steps the effective period leads to infinity, $T_{eff} \rightarrow \infty$, and as well known, for very long period structures the absolute acceleration returns to zero. Hence, the maximum acceleration becomes equal to the maximum recorded during the elastic regime. For hardening materials the effect of damping does not affect the response significantly. An increase of the hardening coefficient leads to a decrease of the difference between the responses based on different damping formulations.

Rayleigh damping is very popular in the analysis of MDOF structures because its implementation is easy and efficient. In general, MDOF structures show positive or negative post yielding stiffness. Exactly zero stiffness in post yielding is a special case and untypical in realistic structures. Therefore, it is not obvious to what extent the aforementioned difference between mass- and stiffness-proportional damping for an SDOF system translates to the MDOF response. Surely, though, the effect will not be as dramatic as in the isolated case of the elastic-plastic system.

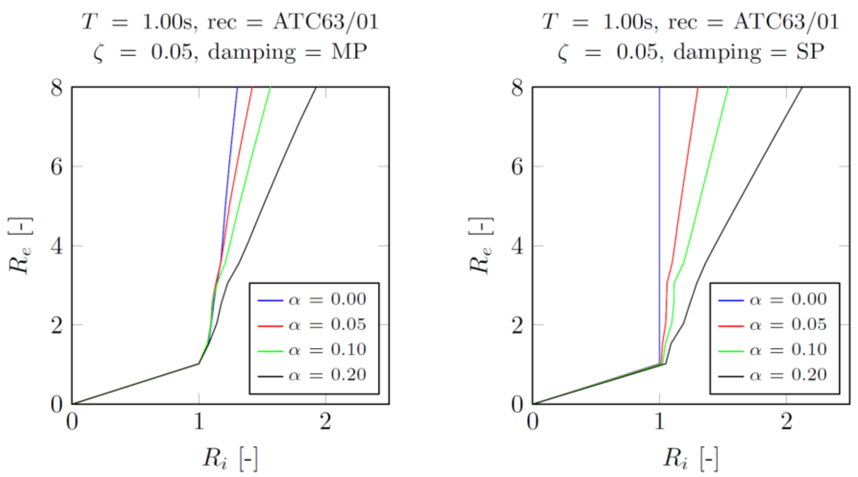

Figure 5. Mass- (left) vs. tangent-stiffness-proportional (right) damping, positive post-yielding.

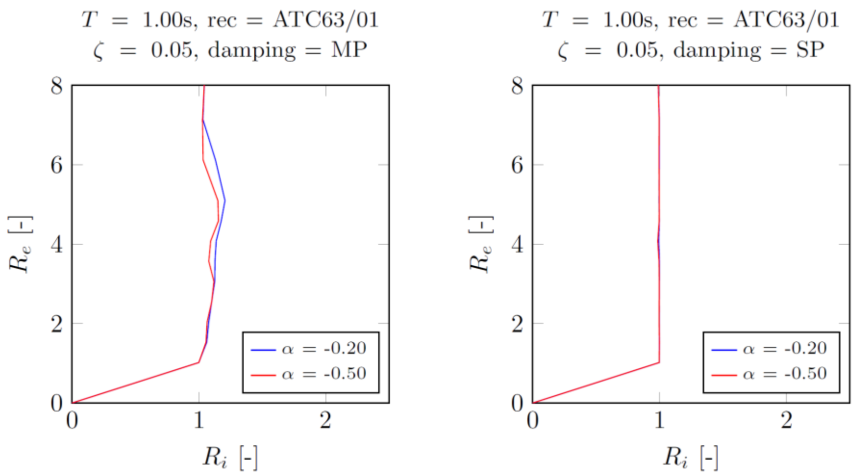

Figure 6. Mass- (left) versus tangent-stiffness-proportional (right) damping, negative post-yielding.

2.1.5 Influence of post-yield softening

In this study the same oscillator model but using negative post yielding stiffness coefficients α = [-0.20, -0.50] is used to perform a single record IDA. A more realistic moderately pinching hysteresis is employed (Ibarra et al. 2005). SEQ shows the effect of different damping types (mass- vs. tangent-stiffness-proportional) on the entire IDA curve. Stiffness-proportional damping shows the same effect for positive as well as negative post-yielding stiffness, because of the direct relation to the stiffness of the oscillator. Mass-proportional damping shows slightly increasing inelastic accelerations with increasing intensity. This comes out because yielding is not happening at the same time for different intensity levels. It seems that inelastic acceleration responses depend on the number of load cycles and on the dissipated energy. Thus, it is difficult to find a qualitative explanation for the shape of the entire IDA curve. Overall, though, it seems to be an adequate approximation to assume that the inelastic peak acceleration is almost equal to the maximum elastic value when the system starts losing strength.

For MDOF structures it is important to note that acceleration does not increase by much, when the structure is completely yielded. This means the critical point, regarding loss estimation, is reached when the capacity curve of the structure turns from positive to negative stiffness. Then loss will be driven by displacement response or by the collapse probability, rather than any increase in acceleration values.

2.2 Multi-degree-of-freedom systems

MDOF systems are modelled using the generic frames provided by Medina and Krawinkler (2003). In these, structural properties are determined by the condition that the first mode shape ϕ_1 is linear and the fundamental period T_1 is proportional to the number of stories N. In this study a flexible six-story moment resisting frame serves as load bearing structure, then the fundamental period leads to T_1 = 1.20 s. Furthermore, is assumed that the bilinear springs (exhibiting 3% strain hardening) located at the base and the girder's ends start yielding simultaneously when applying a lateral force pattern corresponding to the first mode shape. The base shear coefficient is assumed to be γ = 0.10. An IDA is performed for the intensity levels S_a (1.20 s, 5%) = [0.10, 1.00, 5.00] g to figure out profiles of PFAs, see Figure 7. The profiles are normalized to PGA on the horizontal axis, and to the relative height of the structure on the vertical axis. Up to an intensity level of S_a = 0.10 g (blue curves) the structure behaves elastically. With increasing intensity level, PFA decreases. This is clearly shown by the median (bold curves) response quantities, which agree qualitatively with those derived by Miranda and Taghavi (2009). The elastic structure shows maximum PFA at the roof level. With increasing intensity the building becomes more and more inelastic, and maximum PFA returns to PGA at the base. Note that for increasing intensity the profiles translate from left to right. With increasing floor levels PFA decreases, and minimum PFA is approximately between 1/2 and 2/3 of the structure's height.

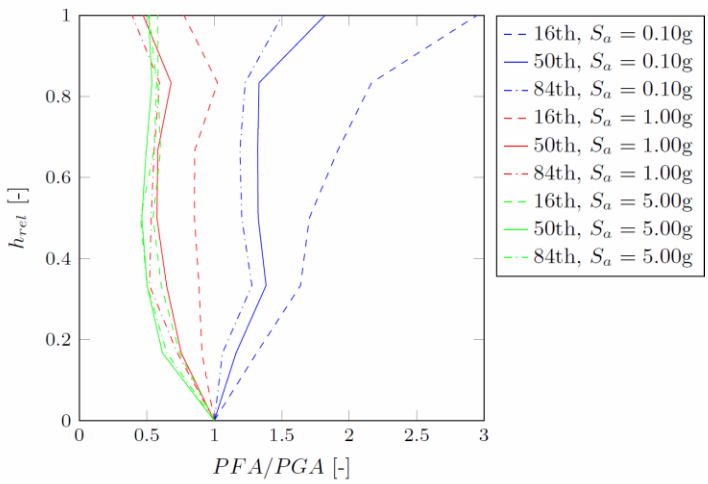

Figure 7. Profiles of peak floor accelerations.

3 APPROXIMATION OF ELASTIC PEAK FLOOR ACCELERATION DEMAND

Several authors propose methods to estimate PFA for linear elastic structures. For steel buildings and reinforced concrete wall frames López-García et al. (2008) proposed a procedure based on modal superposition using either the square-root-of-sum-of-squares (SRSS) method or the complete quadratic combination (CQC) method. Neglecting damping forces simplifies their approach, and lateral effective seismic forces for the sth floor F_s are obtained either by response spectrum analysis or by the equivalent lateral force pattern (ELFP) procedure. Thus, PFA of the sth story is simply the ratio of F_s and the corresponding story mass m_s:

$$PFA_s = \frac{F_s}{m_s}, \quad s = 1, \ldots, N \tag{7}$$

The results show that approximations of SRSS and CQC are generally close. The problem with PFA in comparison to peak floor displacement demands is that each mode is correlated with the base acceleration. An extended CQC method presented by Taghavi and Miranda (2008) takes into account the correlation between modal peak accelerations and PGA:

$$PFA_s = \sum_{j=1}^{N} P_{a_{s,j}} \rho_{g,j} PGA + \sum_{j=1}^{N}\sum_{k=1}^{N} P_{a_{s,j}} \rho_{f,jk} P_{a_{s,k}} \tag{8}$$

where the correlation coefficients are $\rho_{g,j}$ to consider the correlation of jth modal peak acceleration at story s $P_{a_{s,j}}$ with PGA, and $\rho_{f,jk}$ between the jth and the kth modal peak acceleration:

$$\rho_{g,j} = 1 - 1.2e^{-(3.75\zeta + 0.20)\omega^{1.50}}, \quad \rho_{f,jk} = 1 - 1.1e^{-(0.72\zeta + 0.033)\omega^{1.25}} \tag{9}$$

where ω is always the smaller of the jth and kth natural circular frequency, i.e. $\omega = \min[\omega_j, \omega_k]$. A very simple but still efficient method, based on a first mode approximation to estimate PFA in the sth floor, is proposed for the Global Earthquake Model (Porter et al. 2012),

$$PFA_s \approx PGA + \phi_{1,s}(\Gamma_1 S_{ae}(T_1, \zeta) - PGA) \leq PFA_{max} \tag{10}$$

where ϕ_1 is the fundamental mode shape normalized to the maximum response, and Γ_1 is the first mode participation factor. PFA_{max} is the upper limit for PFA related to the structure's strength when the capacity curve turns over to negative stiffness. In the case of the considered six-story generic frame no upper limit exists ($PFA_{max} \to \infty$) because of non-deteriorating material properties, either cyclically or in-cycle.

In Figure 8 the proposed approximation is compared to the IDA results for the first, fourth and the sixth floor (roof). Single record IDAs show the onset of inelasticity at $S_{ae} \approx 0.10$ g. Dispersions of the GEM method come out from the scaled PGA. On the roof floor dispersions equal zero because of the normalization of the first mode shape. The estimation of first floor PFA shows good results. It seems that PGA is what mostly affects the first mode approximation for the GEM approximation.

The outcome agrees with the elastic profiles in Figure 7 where PGA dominates PFA. The higher the floor level the worse the approximation becomes because of the normalization to the roof response of the first mode shape.

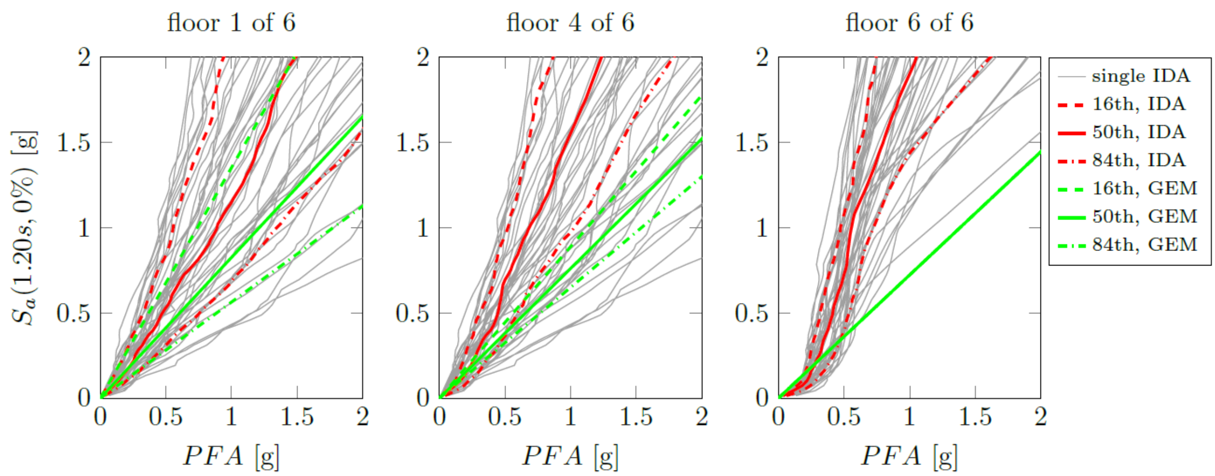

Figure 8. GEM approximation versus IDA.

4 APPROXIMATION OF INELASTIC PEAK FLOOR ACCELERATION DEMAND

To estimate the inelastic peak floor acceleration demand $PFA_{i,s}$ a modification of the GEM method is proposed. Therefore, Eqs (3) and (4) are used to estimate the inelastic peak acceleration P_{ai} , and Eq. (10) becomes:

$$PFA_{i,s} \approx PGA + \phi_{1,s}(\Gamma_1 P_{ai}(T_1,\zeta) - PGA) \tag{11}$$

The advantage of using the inelastic acceleration demand is that no restrictions are needed regarding an upper limit of intensity level. Figure 9 shows the approximation of the inelastic acceleration demand for the first, fourth and sixth floor, respectively (GEM$_i$ in the legend for inelastic approach). The quality of PFA estimation of the first floor leads to good results for central tendency as well as for the dispersions. With increasing number of stories the quality of the inelastic approximation decreases. Note that the parameters to estimate the inelastic acceleration demand of the SDOF system are determined for an elastic-plastic oscillator, rather than utilizing the actual backbone shape of the structure. The global pushover for the six-story generic frame shows a post-yielding stiffness of approximately 1.14%. The estimation would become a little better by considering this. It is important to note that the proposed method depends only on a single mode. Thus, it makes sense to modify this approach and apply an extended modal combination in the next step of this research.

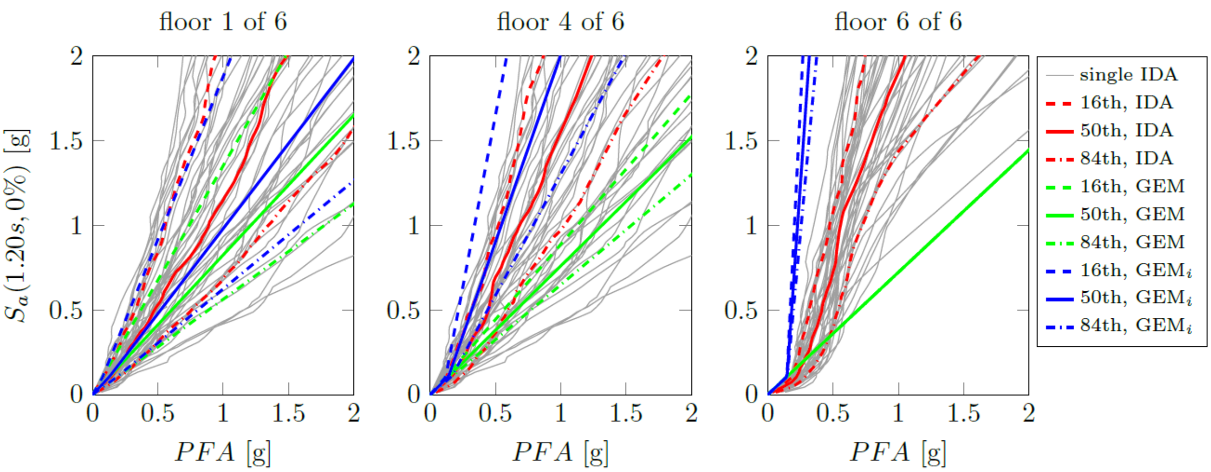

Figure 9. Elastic approximation versus inelastic approximation versus IDA.

5 CONCLUSIONS

In this paper a methodology for estimating the inelastic peak floor acceleration demand has been presented. The elastic-plastic single-degree-of-freedom oscillator excited by the records of the ATC63 far-field record set serves as mechanical model to record peak acceleration demands. Influence of perfectly plastic, hardening and negative post-yielding stiffness on acceleration demand is discussed. Effects regarding mass- and tangent-stiffness-proportional damping on inelastic response are shown, and consequences to multi-degree-of-freedom (MDOF) structures identified.

Regression analysis is used to determine an analytical solution for relationship between elastic spectral acceleration (IM) and inelastic peak acceleration demands (EDP). In a further step, an existing first mode approximation procedure to estimate elastic peak floor acceleration demands of MDOF structures is modified to predict inelastic peak floor accelerations. In terms of loss assessment, professionals need a sufficiently accurate but still effective method to estimate acceleration demands in inelastic structures. The proposed method is applied to a six-story generic frame structure. For a first attempt the approximation shows adequate results, but there is still the need to enhance the methodology in the future and to test it on several lateral-load resisting systems. Extended modal combination methods should lead to better approximations.

ACKNOWLEDGEMENTS

The authors are grateful to Dr. Keith Porter for providing the draft of the Global Earthquake Model before final publication. The second author also acknowledges the support of the GEM Foundation through the GEM Vulnerability Consortium.

REFERENCES

López-García, D., Price, P., Torrejón, E., Vial, F. and Wichmann, P. (2008). Peak floor accelerations in multistory buildings subjected to earthquakes. In: *The 14th World Conference on Earthquake Engineering (14WCEE)*; October 12-17, 2008, Beijing, China. CD-ROM paper, Paper No. 05-01-0313, 8 pp.

Taghavi, S. and Miranda, E. (2008). Response spectrum method for estimation of peak floor acceleration demand. In: *The 14th World Conference on Earthquake Engineering (14WCEE)*; October 12-17, 2008, Beijing, China. CD-ROM paper, Paper No. 313, 9 pp.

Miranda, E. and Taghavi, S. (2009). A comprehensive study of floor acceleration demands in multi-story buildings. In: Goodno, B. (ed.), *Improving the Seismic Performance of Existing Buildings and Other Structures*: pp. 616-626.

Wilson, E.L., Der Kiureghian A. and Bayo, E.P. (1981). A replacement for the SRSS method in seismic analysis. *Earthquake Engineering and Structural Dynamics* **9**: 187-194.

Ruiz-García, J. and Miranda, E. (2007). Probabilistic estimation of maximum inelastic displacement demands for performance-based design. *Earthquake Engineering and Structural Dynamics* **36**: 1235-1254.

Chaudhuri, S.R. and Hutchinson, C.T. (2004). Distribution of peak horizontal floor acceleration for estimating nonstructural element vulnerability. In: *The 13th World Conference on Earthquake Engineering (13WCEE)*; August 1-6, 2004, Vancouver, Canada. CD-ROM paper, Paper No. 1721, 15 pp.

Ibarra, L.F., Medina, R.A. and Krawinkler, H. (2005). Hysteretic models that incorporate strength and stiffness deterioration. *Earthquake Engineering and Structural Dynamics* **34**: 1489-1511.

Limpert, E., Stahel, W.A. and Abbt, M. (2001). Log-normal distributions across the sciences: keys and clues. *BioScience* **51**: 341-352.

Medina, R.A. and Krawinkler, H. (2003). *Seismic demands for nondeteriorating frame structures and their dependence on ground Motions*. Report No. 144. The John A. Blume Earthquake Engineering Center, Department of Civil and Environmental Engineering, Stanford University.

Vamvatsikos, D. and Cornell, C.A. (2005). *Seismic performance, capacity and reliability of structures as seen through incremental dynamic analysis*. Report No. 151. The John A. Blume Earthquake Engineering Center, Department of Civil and Environmental Engineering, Stanford University.

Porter, K., Farokhnia, K., Vamvatsikos, D. and Cho, I. (2012). *Analytical derivation of seismic vulnerability functions for highrise buildings*. Draft. Global Earthquake Model.

ATC-58-1 (2012). *Seismic performance assessment of buildings, Volume 1 – Methodology*. 100% draft. Applied Technology Council.

UBC (1997). *Uniform building code Volume 2 – Structural engineering design provisions*. International Conference of Building Officials.

IBC (2012). *2012 International building code*. International Building Code Council.

ASCE (2006). *ASCE/SEI 7-05: Minimum design loads for buildings and other structures*. American Society of Civil Engineers.

FEMA P-695 (2009). *Quantification of building seismic performance factors*. Applied Technology Council.

FEMA P-750 (2009). *NEHRP recommended seismic provisions for new buildings and other structures*. Building Seismic Safety Council.

EN 1998-1 (2011). *Design of structures for earthquake resistance – Part 1: General rules, seismic actions and rules for buildings*. European Committee for Standardization.